Journal of Solid State Chemistry 197 (2013) 1–6

Contents lists available at SciVerse ScienceDirect

Journal of Solid State Chemistry

journal homepage: www.elsevier.com/locate/jssc

Growth process of $Cu_2Al_6B_4O_{17}$ whiskers

Chengcai Zhu [a,b], Xueying Nai [a], Donghai Zhu [a,b], Fengqin Guo [c], Yongxing Zhang [a,b], Wu Li [a,*]

[a] Qinghai Institute of Salt Lakes, Chinese Academy of Sciences, Xining 810008, PR China
[b] Graduate University of Chinese Academy of Sciences, Beijing 100049, PR China
[c] Department of Basin Education, Qinghai University, Xining 810016, PR China

ARTICLE INFO

Article history:
Received 19 May 2012
Received in revised form
2 August 2012
Accepted 5 August 2012
Available online 23 August 2012

Keywords:
Crystal growth
Whisker
Copper aluminum borate

ABSTRACT

The reactions occurred and growth process in the preparation of copper aluminum borate ($Cu_2Al_6B_4O_{17}$) whiskers based on flux method ($Al_2(SO_4)_3/CuSO_4/H_3BO_3$ as raw materials, K_2SO_4 as flux) were investigated. The thermogravimetric and differential scanning calorimetry analysis (TG-DSC), inductively coupled plasma atomic emission spectrum analysis (ICP-AES) and X-ray diffraction analysis (XRD) results of reactants mixture quenched at various temperatures and phase diagrams of K_2SO_4–$Al_2(SO_4)_3$ system and B_2O_3–Al_2O_3 system showed that the reaction process proceeds through three steps: the formation and decomposition of two different kinds of potassium aluminum sulfate ($K_3Al(SO_4)_3$ and $KAl(SO_4)_2$); the formation of aluminum borate ($Al_4B_2O_9$) and decomposition of copper sulfate ($CuSO_4$) and boric acid (H_3BO_3); growth and formation of copper aluminum borate ($Cu_2Al_6B_4O_{17}$) whiskers. The scanning electron microscopy (SEM) analysis results indicated that morphology in growth of $Cu_2Al_6B_4O_{17}$ whiskers develops through three stages: nanoparticles, fan-shaped whiskers and agminate-needlelike whiskers.

1. Introduction

One-dimensional nanoscale materials, such as nanotubes, nanowires, and nanobelts, have attracted much attention both because of their high tensile property [1,2] and other potential applications. In recent years, inorganic fibers and whiskers have been used mostly as reinforcements in composites and thermal insulation. Various fibrous materials such as glass, carbon, SiC, aluminum borate ($Al_{18}B_4O_{33}$), Al_2O_3, etc., are prepared for such purpose [3]. However, the preparation and application of carbon, SiC and Al_2O_3 whiskers are limited because of the difficult processing method and high cost. The studies of preparations and applications of metal borate whiskers, such as aluminum borate [4–6] and magnesium borate [7–11], are popular research fields in recent years owing to their excellent MOE (modulus of elasticity), intensity and other properties. Most of the metal borate whiskers used as reinforcement in alloy, ceramics are produced by high-temperature sintering [4,12,13]. However, few of researches are focused on reaction and growth process of the whiskers [14].

Copper aluminum borate ($Cu_2Al_6B_4O_{17}$) whisker is a kind of novel double salt borate whisker. The preparation of $Cu_2Al_6B_4O_{17}$ whisker has been reported by us recently [15], but factors affect the preparation of $Cu_2Al_6B_4O_{17}$ whisker, such as heating temperature, heating time, flux type, reactants ratio, reaction process, growth process and so on, need be studied comprehensively in order to prepare $Cu_2Al_6B_4O_{17}$ whiskers effectively and control morphology of $Cu_2Al_6B_4O_{17}$ whiskers. In this contribution, the reaction process and growth process of $Cu_2Al_6B_4O_{17}$ whiskers were researched by X-ray diffraction (XRD), thermogravimetry (TG), plasma spectrometer, SEM and phase diagrams of the $Al_2(SO_4)_3$–K_2SO_4 system and B_2O_3–Al_2O_3 system.

2. Experimental

2.1. Synthesis

All the chemical reagents used in this experiment were of analytical grade and pulverized in grinder. Copper sulfate ($CuSO_4$), boric acid (H_3BO_3), aluminum sulfate octadecahydrate ($Al_2(SO_4)_3 \cdot 18H_2O$), and potassium sulfate (flux, K_2SO_4) powders were used as reagents. These reagents were accurately weighed in a proper amount (Cu:Al:B=2:6:8; total weight 13 g) and the K_2SO_4 addition was 40 wt%. The mixture was further grinded and sieved by 120 mesh screen.

The mixtures were placed in a corundum crucible (50 ml), heated (10 °C/min) to 870 °C and kept for 240 min at 870 °C, then cooled down to room temperature (1 °C/min). During the whole reaction process, samples in different stages were taken out from furnace and quenched with liquid nitrogen (Table 1). As Table 1 shows, samples 1–5 are from heating process, samples 6–8 are

* Corresponding author.
E-mail addresses: zccgn2012@163.com, liwu@isl.ac.cn (W. Li).

0022-4596/$ - see front matter Crown Copyright © 2012 Published by Elsevier Inc. All rights reserved.
http://dx.doi.org/10.1016/j.jssc.2012.08.013

Table 1
Sampling in different reaction stages.

Number	Sampling stage	Temperature (°C)	Thermostatic time (min)
1	Heating	600	0
2		700	0
3		800	0
4		840	0
5		870	0
6	Constant Temperature	870	30
7		870	120
8		870	240
9	Cooling	700	0
10		600	0
11		500	0

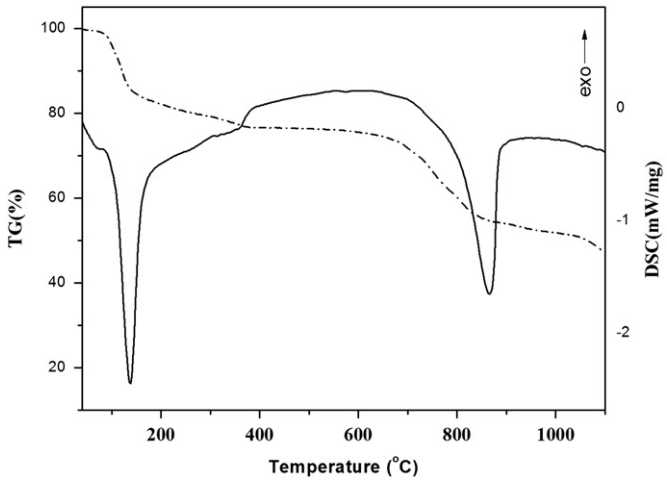

Fig. 1. TG-DSC curve of mixture of the raw materials.

from constant temperature process, samples 9–11 are from cooling process.

2.2. Characterization

The quenched products were identified by X-ray diffraction (XRD, PANalytical X'Pert PRO diffractometer with Cu$K\alpha$ radiation, λ=0.15406 nm), thermogravimetric and differential scanning calorimetry (STA449F3 analyzer) and inductively coupled plasma atomic emission spectrometer (ICAP 6500 DUO). The morphology of the whiskers was characterized by scanning electron microscopy (SEM, JSM-5610LV, JEOL).

3. Results and discussion

3.1. Reaction process

Fig. 1 shows the TG-DSC curve of the mixture of raw materials (Cu:Al:B=2:6:8) and the K_2SO_4 addition was 40 wt%, which was heated from the room temperature to 1100 °C. It is obvious that two different endothermic peaks (138 °C and 866 °C) can be seen in the DSC curve, corresponding to the two different weight loss processes in the TG curve, respectively. In the first stage, H_3BO_3 decomposes and $Al_2(SO_4)_3 \cdot 18H_2O$ dehydrates when the temperature range is 100–400 °C. The weight loss in the temperature range of 100–400 °C is 24.53%, closely corresponding to the theoretical content of water of 25.42%. Few crystal water of $CuSO_4$ dehydrates about 240–320 °C. In the second stage, K_2SO_4 melts as flux at about 750 °C. $CuSO_4$ and $Al_2(SO_4)_3$ break down to activated CuO and Al_2O_3 when the temperature range is 700–950 °C. Two steps exist when $CuSO_4$ is decomposing to CuO and SO_3. First, $CuSO_4$ decomposes to $CuSO_4 \cdot CuO$ and SO_3 from 670 to 820 °C. Then $CuSO_4 \cdot CuO$ decomposes to CuO and SO_3 from 850 to 900 °C [16]. The weight loss in the temperature range of 700–950 °C is 18.71%, closely corresponding to the theoretical content of sulfur trioxide (18.82%). Weight loss of the mixture of the reactants indicates that the temperature ranging from 700 to 950 °C is proper to form $Cu_2Al_6B_4O_{17}$ whisker. However, the TG-DSC results just indicated the weight loss and ex-endothermal process of the mixture, but cannot give the exact composition of intermediate products.

X-ray diffraction (XRD) patterns of quenched samples at different temperatures are described in Fig. 2. All samples were treated by hot water to remove impurities (K_2SO_4). The XRD result in Fig. 2 shows that compound compositions of the intermediate samples are changing along with the calcination temperature and time. Samples 1 and 2 were dissolved absolutely in water. There are four compounds identified by XRD: monopotassium aluminum sulfate ($KAl(SO_4)_2$), tripotassium aluminum sulfate ($K_3Al(SO_4)_3$), aluminum borate ($Al_4B_2O_9$) and copper aluminum borate ($Cu_2Al_6B_4O_{17}$). Only $KAl(SO_4)_2$ and $K_3Al(SO_4)_3$ were observed before 870 °C (samples 3 and 4). At 870 °C, the diffraction peaks of $K_3Al(SO_4)_3$ disappeared and that of the $KAl(SO_4)_2$ existed (sample 5). The intermediate product ($Al_4B_2O_9$) and final product ($Cu_2Al_6B_4O_{17}$) formed gradually at constant temperature process at 870 °C (samples 6–8). Fig. 2 (samples 6–8) shows characteristic peaks of products (2θ): 16.7, 26.6, 33.8 and 43.5. The same characteristic peaks for $Al_4B_2O_9$ and $Cu_2Al_6B_4O_{17}$ mean that the existence of crystal phase transitions from $Al_4B_2O_9$ to $Cu_2Al_6B_4O_{17}$. The result of XRD indicates that $Cu_2Al_6B_4O_{17}$ is derived from $Al_4B_2O_9$. Boric acid and copper sulfate were not detected in the samples even before heating, owing to its relatively low concentration and amorphous forms.

XRD results just identify crystal compound, but some intermediate products, such as CuO, B_2O_3, are still in amorphous forms when quenching from high to room temperature. Fig. 3 shows color change of intermediate products which were treated by hot distilled water to remove water-soluble compounds. In heating

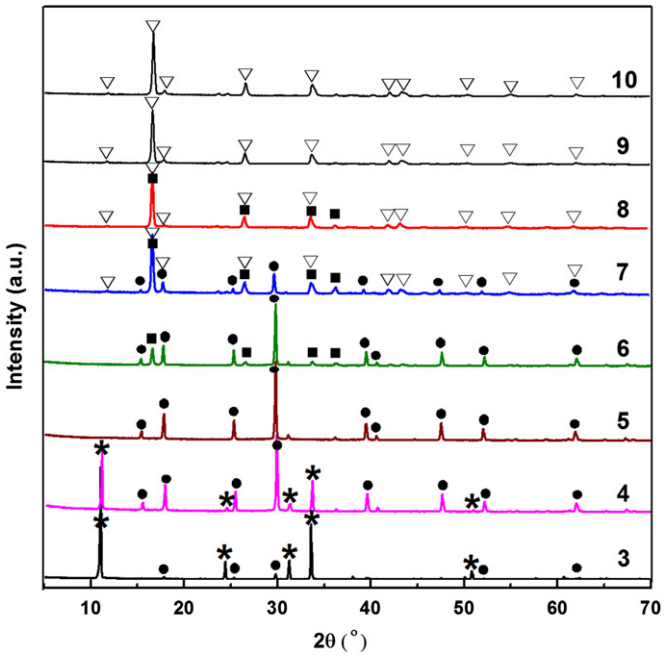

Fig. 2. Composition changes of intermediate product. Sample sequence is corresponding to Table 1. ★—$K_3Al(SO_4)_3$, ●—$KAl(SO_4)_2$, ■—$Al_4B_2O_9$, ▽—$Cu_2Al_6B_4O_{17}$.

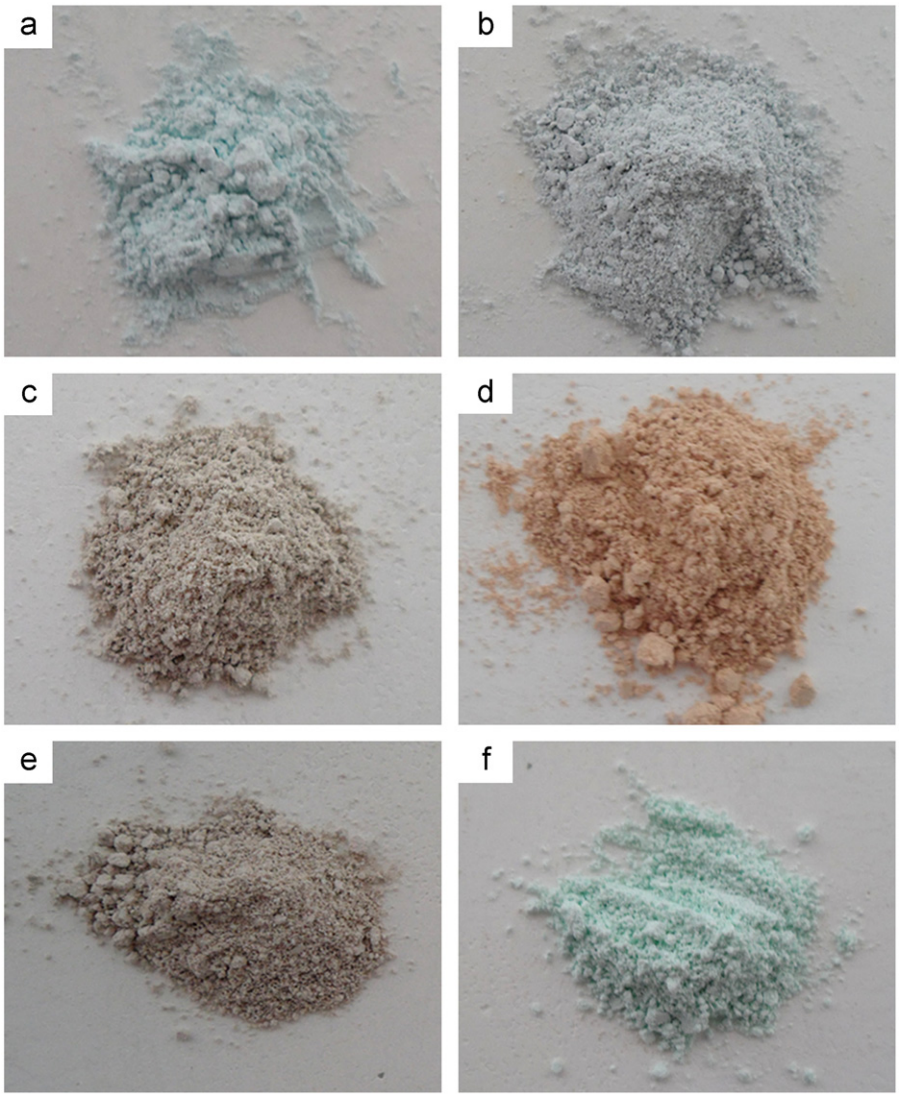

Fig. 3. Appearance of intermediate product at different temperatures and times: in heating process (a) 840 °C; in constant temperature process at 870 °C for (b) 30 min, (c) 120 min, (d) 240 min; in cooling process (e) 600 °C, (f) 500 °C. (For interpretation of the references to color in this figure caption, the reader is referred to the web version of this article.)

process, the product color is sky-blue, corresponds to the color of $CuSO_4$ (sample a). During constant temperature at 870 °C (samples b–d), color changes from gray to erythrine (the color of CuO) and some vitreous products are found (amorphous B_2O_3). In cooling process, color changes from gray to light green (sample f, the color of $Cu_2Al_6B_4O_{17}$). These indicate that amorphous CuO and B_2O_3 exist in the process. However, copper aluminum borate can hardly resolve in dilute hydrochloric acid. To understand the changing law of amorphous compounds of copper (Cu) and aluminum elements, intermediate products are dissolved by dilute hydrochloric acid (0.5 mol/L) and analyzed by plasma spectrometer (Fig. 4). Both copper and aluminum elements increase gradually in the process of heating and constant temperature, but decrease quickly in cooling process. Figs. 3 and 4 confirmed that amorphous compounds of copper (Cu) and aluminum elements reached at the highest value before cooling. Thus, it is concluded that a mass of copper and aluminum elements are consumed in cooling process to supply the growth of whiskers. Moreover, the results predict that appropriate cooling rate is better for reagents and yield of whiskers.

Based on the discussion and results in the XRD and TG-DSC, the reaction process when raw materials were heated can be confirmed by the phase diagrams of $Al_2(SO_4)_3$–K_2SO_4 [17] and

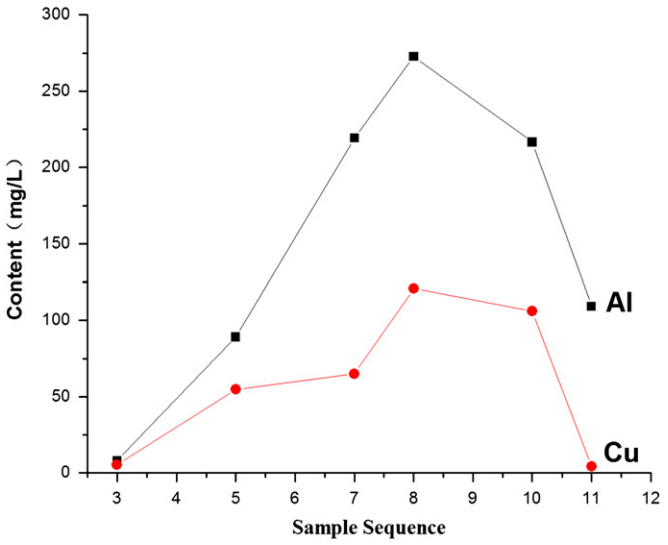

Fig. 4. Amorphous change of Cu and Al in intermediate product. Sample sequence is corresponding to Table 1.

B_2O_3–Al_2O_3 [18]. As shown in Fig. 5, the phase in which the aluminum salts formed and decomposed are different for mixtures with different $K_2SO_4/Al_2(SO_4)_3$ ratios. The change of phase point of mixture (molar ratio of Cu:Al:B as 2:6:8, the K_2SO_4 addition was 40 wt%) at different temperatures is plotted by dotted line on the $Al_2(SO_4)_3$–K_2SO_4 phase diagram. Four different sulfates exist in heating process: K_2SO_4 (below 620 °C), $K_3Al(SO_4)_3$ (527–680 °C), $KAl(SO_4)_2$ (680–780 °C), $Al_2(SO_4)_3$ (780–827 °C), corresponding to the results of XRD (Fig. 2). At 870 °C, $Al_2(SO_4)_3/K_2SO_4$ ratio is decreased slowly because of the formation of $Al_4B_2O_9$ and $Cu_2Al_6B_4O_{17}$. And the phase point moves into liquid–solid phase region of K_2SO_4. According to the result of plasma spectrometer (Fig. 4), the formation of $Al_4B_2O_9$ and $Cu_2Al_6B_4O_{17}$ still exists in cooling process. These indicate that enough thermostatic time and cooling rate are beneficial to conversion of aluminum element.

In order to fully understand the interactions occurring between Al_2O_3 and B_2O_3 it is necessary to study the relevant phase diagram first. From the phase diagram of the Al_2O_3–B_2O_3 system [18] in Fig. 6, it is clear that B_2O_3 reacts with Al_2O_3 to form $Al_4B_2O_9$ and/or $Al_{18}B_4O_{33}$ depending on the composition and temperature. If the ratio of Al_2O_3/B_2O_3 is less than 67% and temperature is between 500 °C and 1150 °C, the most favorable borate phase would be $Al_4B_2O_9$ which then transforms into $Al_{18}B_4O_{33}$ at temperatures above 1150 °C. The phase diagram shows that phase point (molar ratio of Al:B as 3:4) is in liquid–solid phase region of $Al_4B_2O_9$ at 870 °C in this work, consistent with the result of XRD (Fig. 2, samples 6–8).

The TG and XRD results of reactants quenched at various temperatures and phase diagrams of K_2SO_4–$Al_2(SO_4)_3$ showed that the reaction process proceeds through three main steps: the formation and decomposition of potassium aluminum sulfate ($K_3Al(SO_4)_3$ and $KAl(SO_4)_2$); the formation of aluminum borate ($Al_4B_2O_9$) and decomposition of copper sulfate ($CuSO_4$) and boric acid (H_3BO_3); the growth and formation of copper aluminum borate ($Cu_2Al_6B_4O_{17}$) whiskers. According to the above results, the

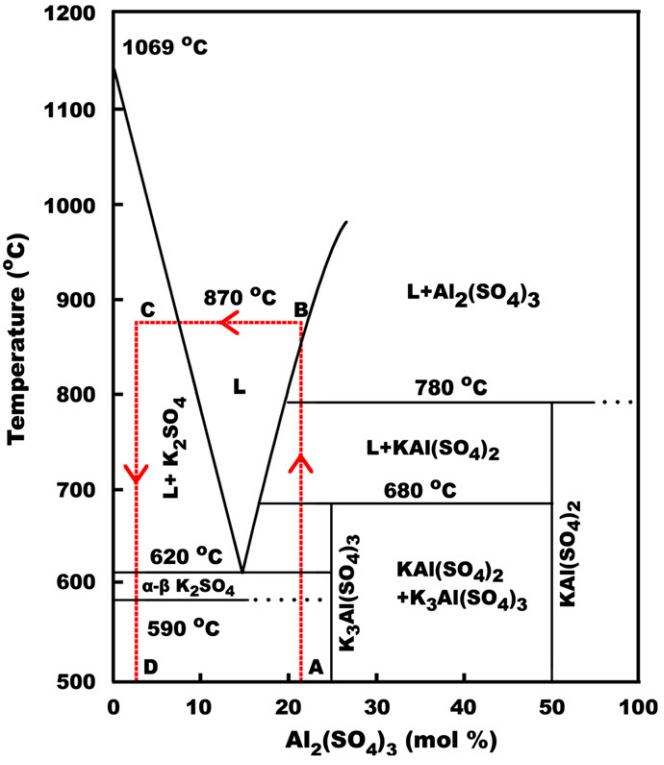

Fig. 5. Phase diagram of K_2SO_4–$Al_2(SO_4)_3$ system [17].

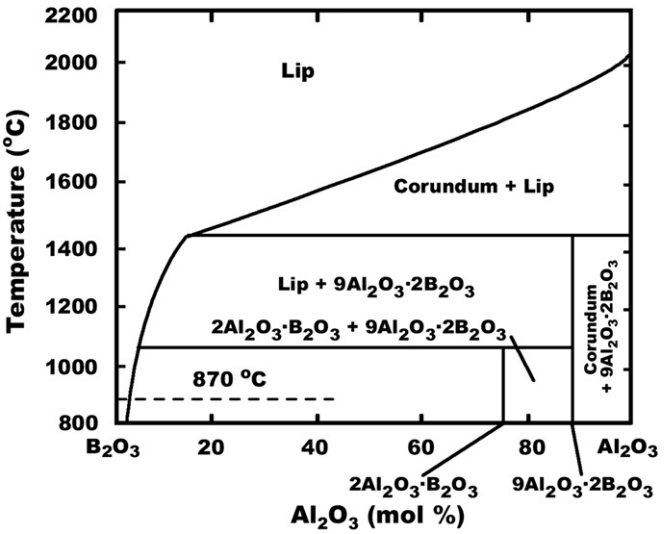

Fig. 6. Phase diagram of B_2O_3–Al_2O_3 system.

reaction mechanism of $Cu_2Al_6B_4O_{17}$ whiskers could be proposed as follows (Eqs. (1)–(8)):

$$2CuSO_4 \rightarrow CuSO_4 \cdot CuO + SO_3 \quad (1)$$

$$CuSO_4 \cdot CuO \rightarrow 2CuO + SO_3 \quad (2)$$

$$2H_3BO_3 \rightarrow B_2O_3 + 3H_2O \quad (3)$$

$$3K_2SO_4 + Al_2(SO_4)_3 \rightarrow 2K_3Al(SO_4)_3 \quad (4)$$

$$K_3Al(SO_4)_3 \rightarrow KAl(SO_4)_2 + K_2SO_4 \quad (5)$$

$$2KAl(SO_4)_2 \rightarrow Al_2O_3 + K_2SO_4 + 3SO_3 \quad (6)$$

$$2Al_2O_3 + B_2O_3 \rightarrow Al_4B_2O_9 \quad (7)$$

$$3Al_4B_2O_9 + 4CuO + B_2O_3 \rightarrow 2Cu_2Al_6B_4O_{17} \quad (8)$$

These equations show that potassium sulfate flux is not only a reaction flux but also a catalyst participating in the reactions. Compared with the frequently used potassium chloride, lower reaction temperature and higher reactivity of alumina are obtained while we use potassium sulfate as flux.

3.2. Growth process of whisker

The quenched products were immersed and washed by hot water and dilute HCl solvent, respectively, to remove residual boric acid, potassium sulfate and other by-products.

The effects of the temperature on the composition and morphology of the intermediate products at different reaction stages are shown in Fig. 7. As shown in Fig. 7, the morphology of products is various in different stages. Only irregular nanoparticles are formed below 840 °C. Particles mixed with fewer fan-shaped whiskers appear when the temperature just reached 870 °C. Fewer particles and tremendous fan-shaped whiskers appeared at 870 °C for 30 min. Accompany with homothermal process, the whiskers grow from fan-shaped to agminate-needlelike. The diameters and lengths of whiskers will no longer change when cooled down below 700 °C. The morphological changes of intermediate products indicate that the growth of whiskers develops through three stages: nanoparticles, fan-shaped whiskers and agminate-needlelike whiskers.

Combined with the above analysis of TG-DSC, XRD, SEM and phase diagrams of the $Al_2(SO_4)_3$–K_2SO_4 system and B_2O_3–Al_2O_3

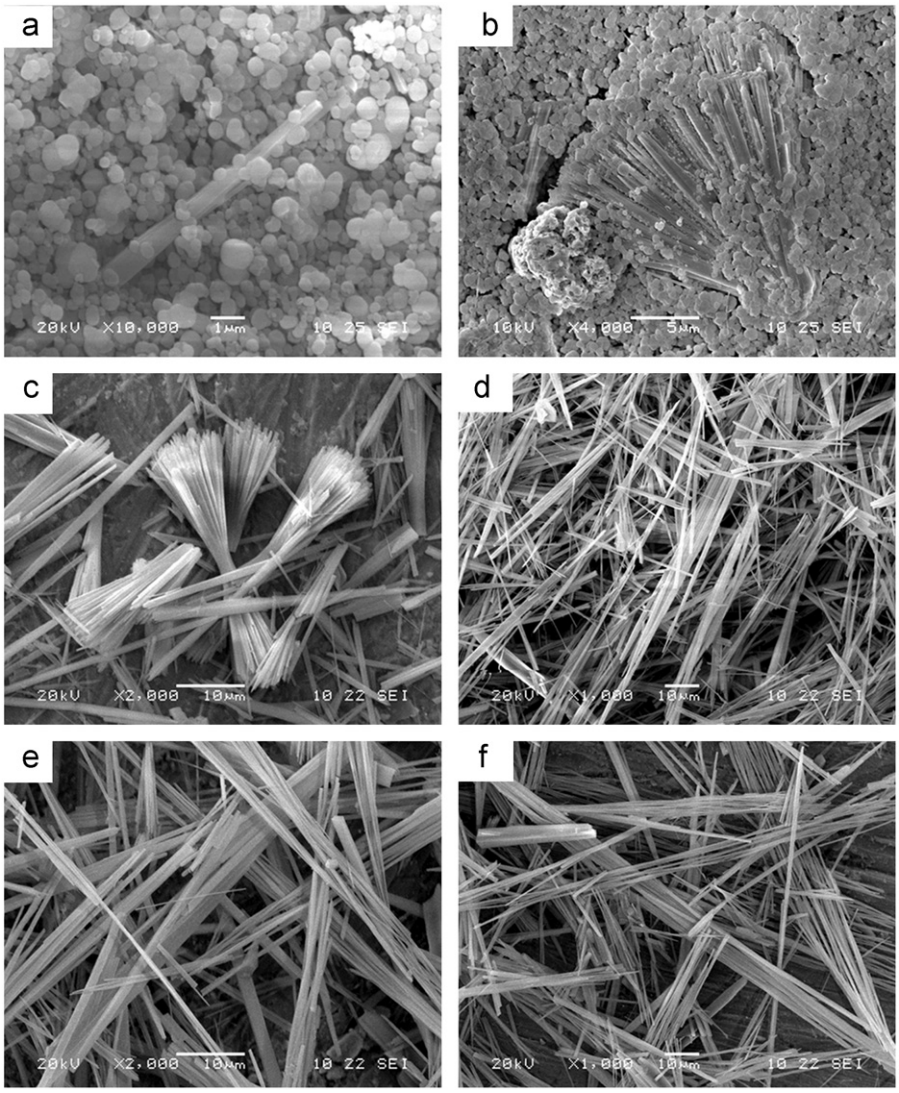

Fig. 7. Morphology of intermediate products (SEM) at different temperatures and times: in heating process (a) 840 °C, (b) 870 °C; in constant temperature process at 870 °C for (c) 30 min, (d) 240 min; in cooling process (c) 700 °C, (d) 600 °C.

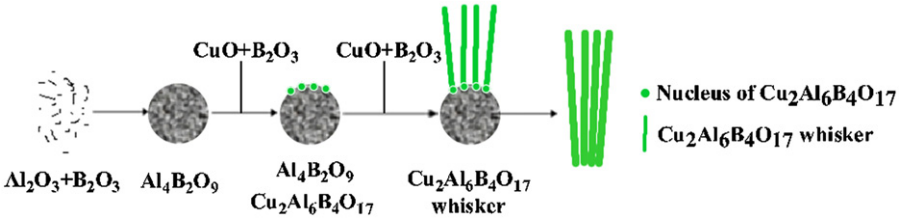

Fig. 8. Growth process of $Cu_2Al_6B_4O_{17}$ whisker.

system, as shown in Fig. 8, the possible growth mechanism of whiskers might be as follows: the crystal phase transitions from aluminium borate ($Al_4B_2O_9$) to copper aluminum borate ($Cu_2Al_6B_4O_{17}$) indicate that fan-shaped whiskers are growing from $Al_4B_2O_9$ particle. Copper aluminum borate ($Cu_2Al_6B_4O_{17}$) nucleates and grows from particle because of the anisotropy and active growing point of $Al_4B_2O_9$. During the whiskers' growth process, $Al_4B_2O_9$ particles are consumed gradually as reaction material until the generation of agminate-needlelike whiskers. Copper oxide (CuO) and boron oxide (B_2O_3) are supplied constantly for the formation of $Cu_2Al_6B_4O_{17}$.

4. Conclusions

In conclusions, the reaction process and possible growth mechanism of $Cu_2Al_6B_4O_{17}$ whiskers were proposed by studying intermediate products in different stages. The results of TG-DSC curve, XRD patterns and plasma spectrometer combined with analysis of phase diagrams of the $Al_2(SO_4)_3$–K_2SO_4 system and B_2O_3–Al_2O_3 system proved that reaction process proceeds through three steps: the formation and decomposition of potassium aluminium sulfate ($K_3Al(SO_4)_3$ and $KAl(SO_4)_2$); the formation of aluminum borate ($Al_4B_2O_9$) and decomposition of copper

sulfate ($CuSO_4$) and boric acid (H_3BO_3); the growth and formation of copper aluminum borate ($Cu_2Al_6B_4O_{17}$) whiskers. From SEM observation, we concluded that the morphology in growth of $Cu_2Al_6B_4O_{17}$ whiskers develops through three stages: nanoparticles, fan-shaped whiskers and agminate-needlelike whiskers.

Acknowledgments

This work was supported by the Qinghai Technology Committee Industorial Public Relation Project of China, Project no. 2010-G-208.

References

[1] R.A. Laudise, The Growth of Single Crystals, Prentice-Hall, Englewood Cliffs, 1970.
[2] A. Parvizi-Majidi, Whiskers and Particulates, Pergamon, Oxford, 2000.
[3] K. Byrappa, M. Yoshimura, Handbook of Hydrothermal Technology—A Technology for Crystal Growth and Materials Processing, 2001.
[4] E.M. Elssfah, H.S. Song, C.C. Tang, J. Zhang, X.X. Ding, S.R. Qi, Materials Chemistry and Physics 101 (2007) 499–504.
[5] Y. Li, R.P.H. Chang, Materials Chemistry and Physics 97 (2006) 23–30.
[6] I. Carazeanu, V. Ciupina, C. Guguta, G. Prodan, Microchimica Acta 147 (2004) 147–150.
[7] S.H. Chen, P.P. Jin, G. Schumacher, N. Wanderka, Composites Science and Technology 70 (2010) 123–129.
[8] A.F. Qasrawi, T.S. Kayed, A. Mergen, M. Guru, Materials Research Bulletin 40 (2005) 583–589.
[9] B. Xu, T. Li, Y. Zhang, Z. Zhang, X. Liu, J. Zhao, Crystal Growth & Design 8 (2008) 1218–1222.
[10] U. Dosler, M.M. Krzmanc, D. Suvorov, Journal of the European Ceramic Society 30 (2010) 413–418.
[11] W. Zhu, Q. Zhang, L. Xiang, S. Zhu, CrystEngCommunity 13 (2011) 1654–1663.
[12] J. Wang, G.L. Ning, Y. Lin, Materials Letters 62 (2008) 2447–2449.
[13] J. Wang, G.L. Ning, X.F. Yang, Z.H. Gan, H.Y. Liu, Y. Lin, Materials Letters 62 (2008) 1208–1211.
[14] H. Wada, K. Sakane, T. Kitamura, H. Hata, Journal of Materials Science 31 (1996) 537–544.
[15] Chengcai Zhu, Wu Li, Xueying Nai, Donghai Zhu, Fengqin Guo, Shuangjie Song, Crystal Research and Technology 47 (2012) 73–78.
[16] B.L. Huang, Mineral Differential Thermal Analysis and Appraisal Manual. Science Press, Beijing, PR China, 1987.
[17] L.A. Kochubei, E.V. Margulis, M.M. Shokarev, N.V. Portvelova, Russian Journal of Inorganic Chemistry 23 (1978) 1255.
[18] P.J. Gielisse, W.R. Foster, Nature 195 (1962) 69–70.